Solid Freeform Fabrication 2022: Proceedings of the 33rd Annual International Solid Freeform Fabrication Symposium – An Additive Manufacturing Conference
Reviewed Paper

MATERIAL MODELLING OF THE PHOTOPOLYMERS FOR ADDITIVE MANUFACTURING PROCESSES

K. Sekmen*, T. Rehbein†, M. Johlitz†, A. Lion†, and A. Constantinescu*

* Laboratoire de Mécanique des Solides, CNRS, École Polytechnique, Institut Polytechnique de Paris, 91128, Palaiseau, France
† Department of Aerospace Engineering, Institute of Mechanics, Bundeswehr University Munich, 85577, Neubiberg, Germany

Abstract

Ultraviolet (UV) curing of polymers is a key phenomenon for several additive manufacturing technologies. This contribution presents a model relating the process parameters of UV light intensity and temperature to the thermal and mechanical properties of the polymer and the experimental results used to calibrate the model. Moreover, photo-differential scanning calorimetry (photo-DSC) measurements are performed to investigate the crosslinking reaction and to model the degree of cure as a function of the light intensity and temperature. The viscoelastic properties are measured by UV rheometry and it is shown that the classical time-cure superposition principle can equally be applied to the experimental results. Complete curing and mechanical model equations are provided to describe the material behavior as a result of our experimental findings.

Keywords: Additive manufacturing, UV curing, photopolymer, reaction kinetics, viscoelastic modelling

Introduction

Polymer-based additive manufacturing (AM) opens up new possibilities for the design freedom by enabling the rapid and high-resolution manufacturing of geometrically complex structures that can be tailored for a wide range of applications. Among polymer-based AM technologies, the photopolymerization method is widely utilized as a complex and physical process for the fabrication of highly crosslinked polymer products, in which a curing reaction is initiated by photoexcitation, typically from an ultraviolet (UV) light source. Photopolymerization-based 3D printing technologies differ according to the pattern formation principle, operating systems, and method of layer deposition, such as stereolithography apparatus (SLA) [1, 2], digital light processing (DLP) [3, 4], polyjet printing (PJP) [5, 6], two-photon lithography (TPL) [7, 8] and UV light assisted direct ink writing (DIW) [9, 10] and continuous liquid interface production (CLIP) [11, 12].

Photocurable resins play a significant role in photopolymerization-based 3D printing systems. A motivation for both academic and industrial research is the demand for functional materials that are compatible with existing or newly developed technologies. Fast curing under ambient temperature, low energy consumption, solvent-free formulation as well as spatial and temporal control over photopolymerization are of great interest in a variety of practical applications, such as dental materials [13, 14], fashionwear manufacturing [15, 16], coating [17, 18], tissue engineering [19, 20], metamaterials [16, 21] and microfluidic devices [22, 23].

Despite decades of industrial use of photopolymerization-based 3D printing technology, there are still a number of challenges to be resolved in order to develop reliable and experimentally validated models for the design of printed parts. The relationships between process parameters and thermal and mechanical properties are still not fully established. In order to tackle the insufficient repeatability and consistency in the final products, the correlations of process parameters with both the crosslinking reaction and the mechanical response of UV-cured polymers must be accurately described by phenomenological and constitutive models and fitted to experimental data.

The present work aims to examine the curing kinetics of a commercial photosensitive resin and to combine the degree of cure with viscoelastic properties. The effects of UV light intensity and ambient temperature on the crosslinking behavior are investigated with the photo-differential scanning calorimetry (photo-DSC). A phenomenological model is proposed to model the evolution of the degree of cure during the photopolymerization reaction. In-situ monitoring of the photocuring reaction is also conducted by UV rheometry in order to determine the evolution of the degree of cure-dependent viscoelastic properties. Time-cure superposition principle is applied to the experimental results. To represent the experimental data, the material model parameters for reaction kinetics are identified.

Experimental investigation

Photo-DSC measurements

Crosslinking reactions initiated by heat or UV radiation transform liquid monomers and oligomers into solid polymers. This implies that the monomers that are linked to polymer chains undergo an exothermic reaction. Photo-DSC can analyze the heat released to establish a link between temperature and certain physical properties, allowing it to identify key parameters of the photopolymerization process such as degree of cure, photopolymerization rate and reaction enthalpy as a function of UV light intensity, exposure time and temperature.

Photo-DSC measurements are performed using the TA Instruments DSC Q2000 (TA Instruments, New Castle, DE, USA) with an additional light source (OmniCure® S2000) to understand and investigate the crosslinking process of commercial photopolymers used in additive manufacturing processes. This UV light source has a 200 W high-pressure mercury lamp with a standard filter at a wavelength of 405 nm. The commercial photopolymer PR48 resin is supplied by Colorado Photopolymer Solutions (Boulder, CO, USA) for the measurements. The PR48 is an acrylate-based photopolymer resin that works with 3D printing technologies such as digital light processing (DLP) and stereolithography apparatus (SLA).

The DSC measures the specific heat flow $\dot{h}$ between a sample in a pan and an empty reference pan during the crosslinking reaction over time t in order to investigate the reaction kinetics. The specific heat flow is converted into the degree of cure using Eq. 1 [24]:

$$q(t) = \frac{\int_0^t \dot{h}(\tilde{t})\mathrm{d}\tilde{t}}{h_{tot}} \tag{1}$$

The integration of the accumulated area between the specific heat flow and the abscissa in Eq. 1 represents the heat released by the photopolymer sample during the exothermic reaction, which can be transformed into the degree of cure. The degree of cure is a non-dimensional quantity ranging from 0 (liquid monomer) to 1 (fully cured solid polymer) as it is normalized to the maximum specific heat h_{tot} during the crosslinking reaction.

During the photocalorimetry measurement, the following procedure is performed to determine the specific heat flow $\dot{h}(\tilde{t})$ in Eq. 1: (i) a 2-minute stabilization step of the measurement cell at a specific constant temperature (θ = 10, 20, 30, 40, 50, and 60 °C), (ii) a 10-minute isothermal step of the irradiation of the specimen at a constant UV light intensity (I = 5, 10 mW/cm^2), and (iii) a 2-minute final isothermal step at the specified constant temperature. The curing reaction is considered finished at each isothermal test for a given temperature and incident light intensity when the heat flow curve remains stable over time. After finishing the third step, the whole procedure is repeated with the polymerized sample to generate the baseline heat flow caused by UV absorption between the reference aluminum pan and the polymerized sample. To eliminate the effect of the UV light source, this generated baseline is subtracted from the heat flow signal of the first measurement.

An additional measurement at non-isothermal temperature is performed to determine the maximum specific heat h_{tot} during the crosslinking reaction. The photo-DSC runs are kept isothermally at 60 °C for 2 minutes and then exposed to the UV light with a light intensity of 20 mW/cm^2 for 10 minutes under isothermal conditions. Following that, a non-isothermal step is performed with the same continuous and constant UV irradiation from 60 °C to 120 °C at a heating rate of 20 °C/min. The final step is to perform a 2-minute isothermal DSC scan at 120 °C without UV irradiation. Finally, the same procedure is repeated with the cured polymer. The maximum specific heat generated by this process, h_{tot} = -404.43 J/g, is used as the reference value for all measurements for the conversion of the specific heat generated during the crosslinking reaction into the degree of cure.

After subtracting the baselines, the series of photopolymerization measurements are shown in Fig. 1. It is evident that, after the UV light irradiation starts, the curing reaction progresses very rapidly, particularly at the beginning of the UV irradiation, and that the specific heat flow only takes a few seconds to reach its maximum level. Furthermore, it can be seen that higher temperature and light intensity result in higher maximum values in the exothermic peaks and a faster curing reaction. Additionally, as shown in Fig. 3, complete curing is not achieved at low temperatures and light intensities, and the crosslinking reaction is prematurely stopped.

Table 1 shows the maximum attainable degrees of cure $q_{\max}$ for all measurements. It can be seen that a nearly fully cured material is obtained at a temperature of 60 °C, regardless of the UV light intensity. This result must be considered when developing the material model for the degree of cure.

Table 1: Temperature- and UV light intensity-dependent maximum attainable degree of cure $q_{max}(I, \theta)$ for all measurements.

	10 °C	**20 °C**	**30 °C**	**40 °C**	**50 °C**	**60 °C**
$I = 5$ mW/cm^2	0.635	0.757	0.829	0.893	0.951	0.961
$I = 10$ mW/cm^2	0.742	0.813	0.872	0.918	0.961	0.966

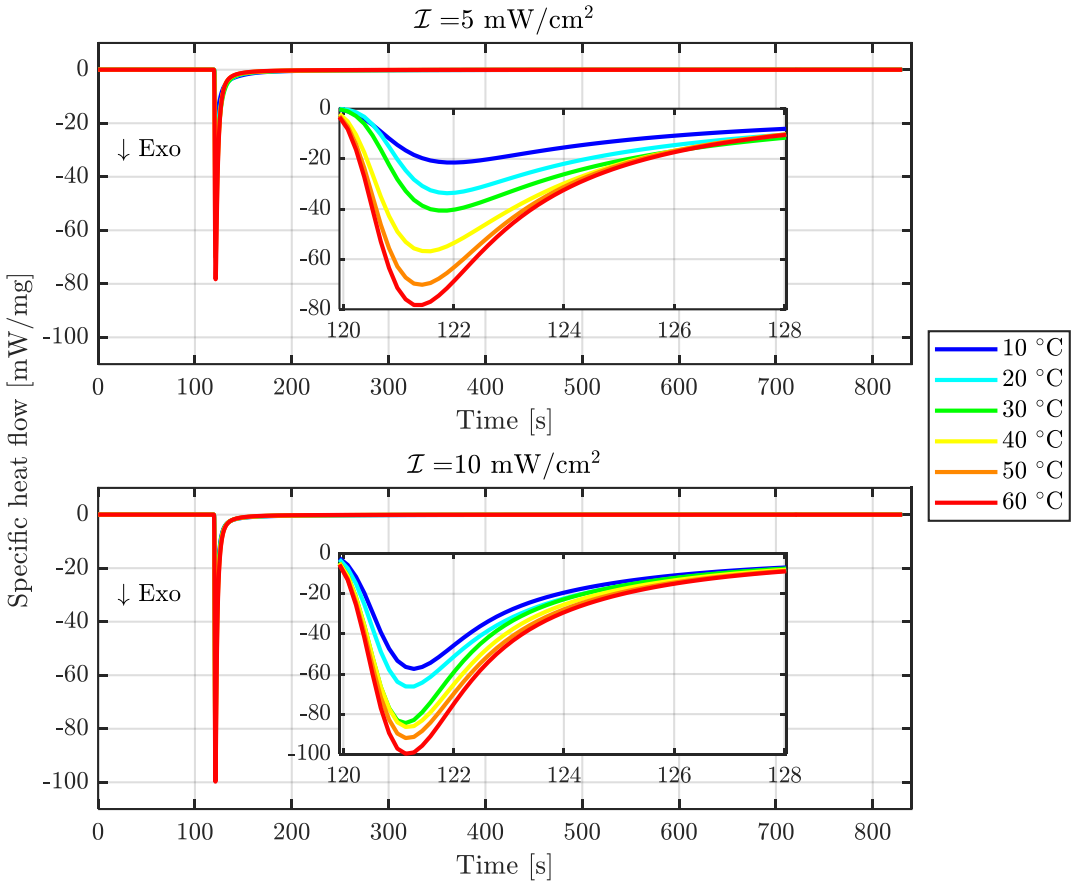

Figure 1: Measured specific heat flows under different isothermal conditions and different UV light intensities.

UV rheometry measurements

UV rheometry measurement is a convenient method for monitoring the evolution of viscoelastic properties in the gel-sol transition of a photopolymer resin in real-time. In this experimental setup, the liquid resin is sandwiched between glass-contained parallel plates in a gap of several hundred micrometers d_{gap} [25]. The sinusoidal shear excitation given in Eq. 2 is first applied to the photopolymer layer at constant frequency $f = 2\pi/\omega$, constant strain amplitude, and isothermal condition over time [26]:

$$\gamma = \hat{\gamma} \sin(\omega t) \tag{2}$$

where ω is the angular frequency and $\hat{\gamma}$ % is the strain amplitude. The UV light irradiation is then activated from the bottom of the glass plate to crosslink the liquid resin while maintaining oscillatory shear excitation. The solidification process starts at the glass plate placed on the bottom and progresses vertically upwards. The UV rheometer can measure the time-dependent change in viscoelastic behavior when the cured photopolymer contacts the top plate.

The evolution of the viscoelastic properties of PR48 resin during photopolymerization reaction is investigated using a hybrid rheometer Discovery HR-3 (TA Instruments, New Castle, DE, USA) equipped with the same light source as used for the photo-DSC measurements. A parallel-plate measuring system with a glass plate and a disposable steel top plate with a diameter of 20 mm is used. The measurement gap is set to $d_{gap} = 500$ µm. For all tests, the UV light intensity is set to $I_0 = 10.12$ mW/cm^2 at the top surface of the glass plate. The rheological properties are measured in auto-strain mode with an initial strain amplitude of gamma $\hat{\gamma} = 0.1$ %. The auto-strain adjustment is utilized to improve signal quality throughout the measurements because the optimal measurement conditions for a liquid material differ from those for a rigid solid. Time sweep tests are carried out for 400 seconds at various constant frequencies ($f = 0.1$, 1, 10, 100 Hz), constant UV intensity, and isothermal temperature ($\theta = 20$ °C). For all tests, the onset time of UV irradiation is set to 60 seconds. Fig. 2 shows the experimental results of the change in the shear storage modulus G' for frequency values of four orders of magnitude. All measurements reveal a rapid increase in the presence of UV irradiation, as well as different evolution of the shear storage moduli due to frequency dependency. After about 120 seconds, the shear storage moduli reach a plateau for all measurements as the curing reaction progresses.

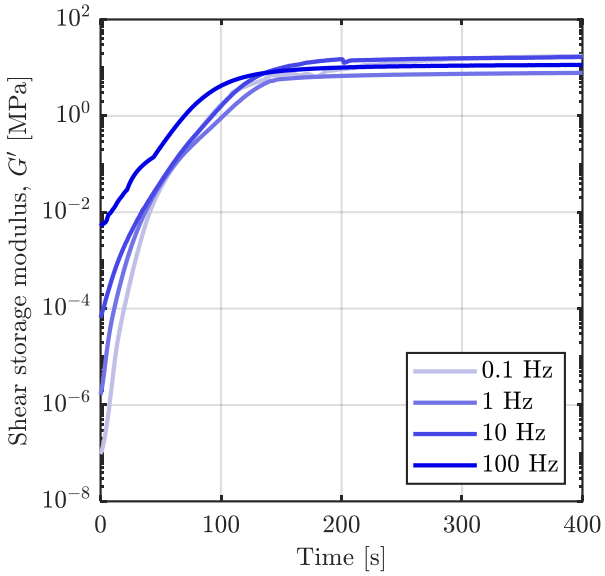

Figure 2: Evolution of the shear storage moduli during the UV rheometry tests under the different frequencies.

Results and Discussion

Modelling of the crosslinking reaction

An autocatalytic model is widely used to describe polymerization reaction kinetics as a function of time and temperature in order to model the evolution of the degree of cure q [27, 28]. Rehbein et al. [24] used an $(m + n)^{th}$ order phenomenological equation based on the autocatalytic kinetic model of Kamal and Sourour [29, 30] and combined it with the work of Maffezzoli and Terzi [31] to account for light intensity. An ordinary differential equation is used to calculate the degree of cure as a function of UV exposure time t, as shown in Eq. 3:

$$\dot{q} = (k_1(I,\theta) + k_2(I,\theta)q^m)(q_{\max}(I,\theta) - q)^n \tag{3}$$

In this model, the degree of cure depends on the time- and location-dependent UV light intensity $I(z(t),t)$ in mW/cm^2 and the ambient temperature θ in °C, as well as the temperature- and UV light intensity-dependent maximum attainable degree of cure $q_{\max}$. The UV light intensity must depend on the vertical direction $z(t)$ because it evolves during the bottom-up printing process. k_1 and k_2 in this equation denote the temperature- and UV light intensity-dependent Arrhenius functions given in Eq. 4:

$$k_i = A_i \exp\left(-\frac{E_i}{RT}\right)\left(\frac{I}{I_{ref}}\right)^b \tag{4}$$

where E_i are activation energies, $R = 8.314$ J/(mol.K) is the universal gas constant, T is the absolute temperature in Kelvin, I_{ref} = 1 mW/cm^2 is a reference value used to ensure the unit consistency of pre-exponential factors A_i in s^{-1}, and b is used to more accurately match the experimental data.

The parameters in Eqs. 3 and 4 are identified using the combination of the nonlinear least-squares data fitting functions of Matlab's built-in routines [32], `lsqnonlin` and `lsqcurvefit` with the Levenberg-Marquardt algorithm and the `ode45` solver. The optimized parameter set is listed in Table 2.

Fig. 3 depicts a comparison between the experimental measurements and the simulations of the degree of cure according to the curing model defined by Eqs. 3 and 4. The proposed model shows a good agreement with the experimental data for all measurement conditions. In particular, the rapid increase in the degree of cure in the first seconds of UV irradiation and the evolution of the degree of cure with ambient temperature, in general, are well represented using only 7 model parameters.

Table 2: Identified parameters of the model equation for the degree of cure q.

A_1	A_2	E_1	E_2	m	n	b
0.135 s^{-1}	0.237 s^{-1}	2003.184 J/mol	2005.08 J/mol	1.848	2.2	0.627

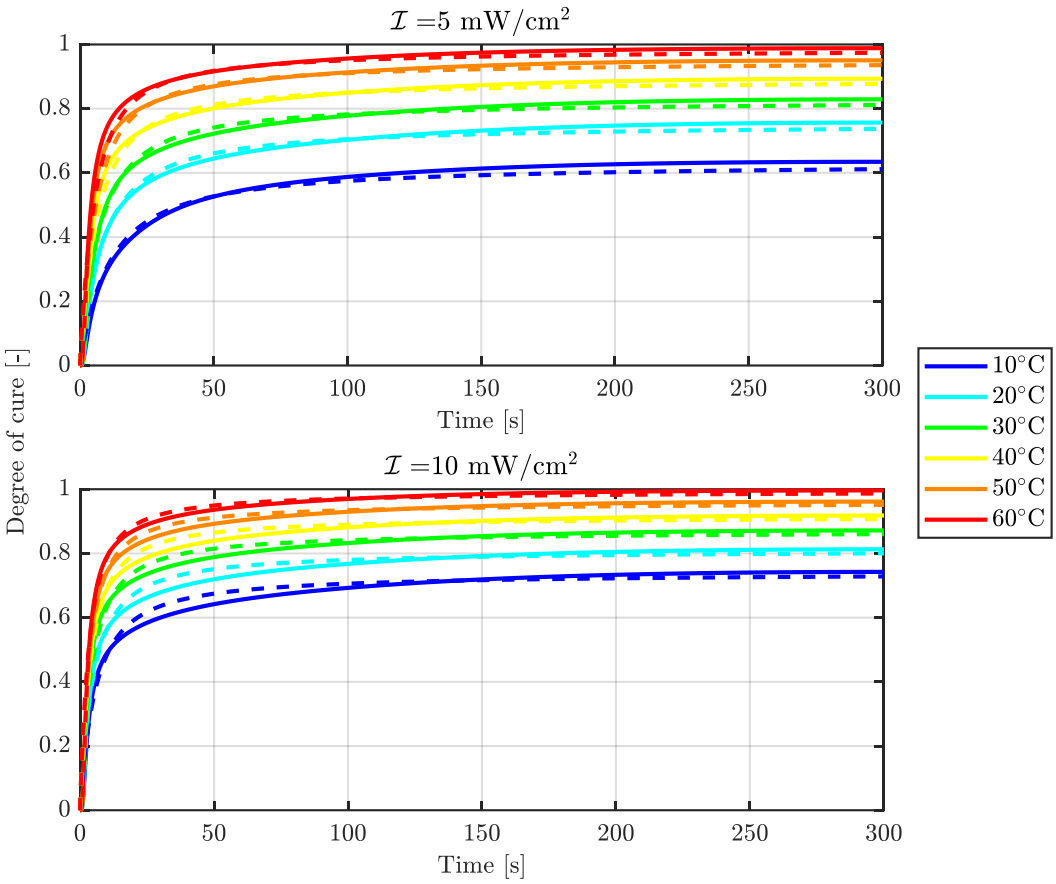

Figure 3: Experimental results of the photo-DSC measurements (—) and simulation with the model equation of the evolution of the degree of cure q (- -).

The total of the mean squared errors (MSE) of all objective functions is determined to measure the quality of the identified model parameters:

$$MSE = \sum_{i=1}^{12} \left(\frac{1}{M} \sum_{j=1}^{M} \left(q_{ij,exp} - q_{ij,sim}(\boldsymbol{x}) \right)^2 \right) \tag{5}$$

where the vector $\boldsymbol{x}$ and scalar value M represent the design space factor, which includes the model parameters for the degree of cure (A_1, A_2, E_1, E_2, b, m, and n) and the number of regression points, respectively. All 12 measurements given in Fig.1 are considered objective functions for the parameter identification procedure represented by the iteration index i. Each MSE is evaluated using a total of $M = 12000$ regression points. The parameters in Table 2 provide the best result of the parameter identification procedure with a summarized MSE of all objective functions of 0.0016.

Time-cure superposition during the photopolymerization reaction

The experimental results in the time domain are linked to the model equations for the degree of cure for the specified test conditions once the shear storage modulus is measured. In order to establish this relationship, the evolution of the degree of cure during the UV rheometry test is calculated using Eqs. 3 and 4, $q_{\max}$ value given for $I = 5$ mW/cm^2 and $\theta = 20$ °C in Table 1 and identified parameters in Table 2. For the UV light intensity, the average value between the parallel plates is used. In order to determine the average light intensity I_{av}, the average function value as given in Eq. 6 is employed, with the Beer-Lambert law given in Eq. 7 [33] and the identified UV curing properties detailed in the previous article [34]:

$$I_{av} = \frac{1}{d_{gap}} \int_0^{d_{gap}} I(z) dz \tag{6}$$

$$I(z) = \exp\left(-\frac{z}{D_p}\right) I_0 \tag{7}$$

where $I(z)$ is the light intensity as a function of distance z, $D_p = 223.2$ µm denotes the penetration depth and $I_0 = 10.12$ mJ/cm^2 is the UV light intensity on the glass plate. The average light intensity is calculated as $I_{av} = 4.04$ mJ/cm^2. The evolution of the degree of cure is then estimated using all of the test parameters for UV light exposure time t, light intensity I_{av} and ambient temperature θ. The experimental findings in the time domain are coupled with the evolution of the degree of cure as proposed in the previous article [35]. As can be seen in Fig. 4, this coupling results in several subcurves of the shear storage modulus dependent on the degree of cure in the frequency domain.

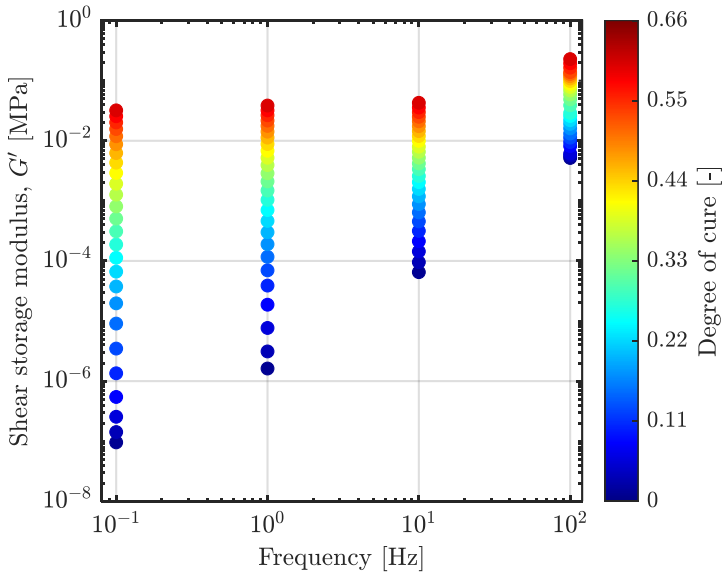

Figure 4: Transformation of the $G' - t$ curves in Fig. 2 into the frequency domain using the model equation of the degree of cure (Eq. 1) at various constant degrees of cure q.

These subcurves in the frequency domain are then manually shifted to generate a master curve at the chosen reference degree of cure $q_{ref} = 0.528$, as shown in Fig. 5. The base 10 exponents of the shift factors used to derive the master curve are presented in Fig. 6.

In order to express the shift factor mathematically, the range of the degree of cure is divided into two parts, before and after the transition of the photopolymer from a fluid into a solid. This transition state is observed at the degree of cure at the gel point (q_{gel}) around 0.32 (Fig. 6). This corresponds to the gelation point determined using ASTM standard D4473 [36] in which the gel point (t_{gel}) is defined as the point as the storage (G') and loss modulus (G'') crossover point under a constant frequency of $f < 1.5$ Hz. The time point of the gel point is determined by measuring the evolution of the viscoelastic material properties (G' and G'') at $f = 1$ Hz versus UV exposure time using UV rheometry. The degree of cure at the gel point is calculated as $q_{gel} = 0.32$ using the model equation of the degree of cure with the test parameters, i.e. UV light intensity, temperature and exposure time.

In the degree of cure range from 0 to q_{gel}, the shift factor is represented as a function of degree of cure by a linear equation, similar to the work of Eom et al. [37], and after gelation, the dependence of the shift factor on the degree of cure is described by a quadratic polynomial function:

$$s_q(q) = \begin{cases} s_{q1}q + s_2\,, & q < q_{gel} \\ s_{q3}q^2 + s_{q4}q + s_{q5}\,, & q \geq q_{gel} \end{cases} \tag{8}$$

where s_{q1}, s_{q2}, s_{q3}, s_{q4} and s_{q5} are dimensionless model parameters determined by Matlab and given in Table 3. The identification result, shown in Fig. 6, indicates a good representation of the time-cure shift factors using Eq. 8.

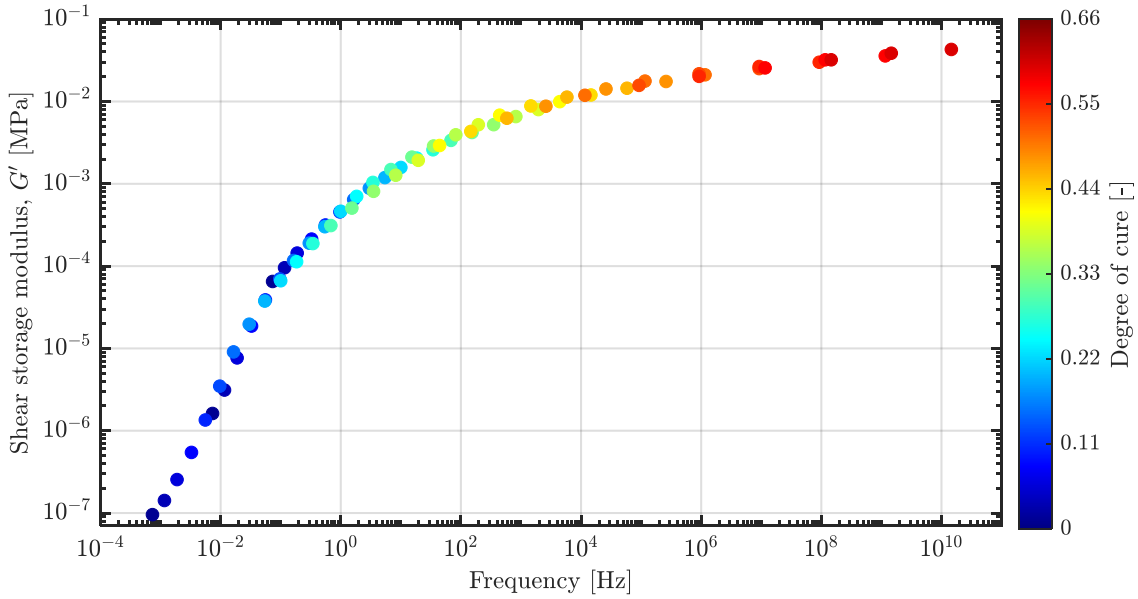

Figure 5: Resulting master curves after shifting the subcurves of Fig. 4 at a constant degree of cure $q_{ref} = 0.528$.

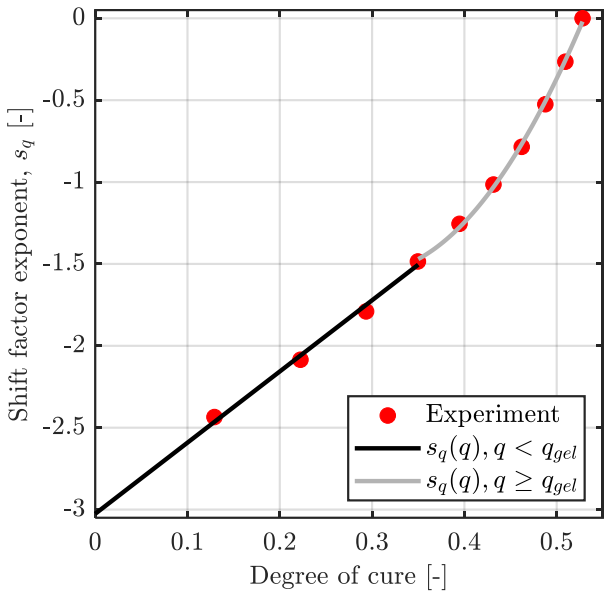

Figure 6: Time-cure shift factors from experimental results and fitting using Eq. 8.

Table 3: Parameters of the time-cure shift functions $s_q\ (q)$.

θ in °C	s_{q_1}	s_{q_2}	s_{q_3}	s_{q_4}	s_{q_5}
20	4.247	-3.026	28.54	-16.91	0.952

Conclusion

This work proposes a thermo-mechanical model for the UV curing of polymers and offers a new perspective on the comprehensive quantitative characteristics needed for the prediction of material properties during the photopolymerization reaction using experimental methods. To determine the material properties, the degree of cure of the material is employed as an internal variable. An autocatalytic relation is used to represent the evolution of the degree of cure assessed by photo-DSC. UV rheology measurements combined with the photo-DSC results indicate that the viscoelastic properties of the photopolymer are strongly dependent on the degree of cure during the crosslinking reaction. The developed modelling framework provides a useful insight to design components for photopolymerization-based 3D printing, hence improving production efficiency and material characteristics.

Forthcoming considerations can be exploited to examine the influence of UV light intensity, temperature and frequency on the viscoelastic properties and chemical shrinkage for the complete photopolymerization process. A finite element (FE) simulation approach can be implemented to improve the printing process by coupling the effects of all relevant physical, mechanical and chemical mechanisms.

Acknowledgement

The authors gratefully acknowledge the Agence nationale de la recherche (ANR) and the German Research Foundation (DFG) for the financial support of the project “Constitutive modelling of UV-curing printed polymer composites" under the grant numbers ANR-18-CE92-0002-01 and LI 696/20-1.

References

[1] J. W. Halloran, “Ceramic stereolithography: additive manufacturing for ceramics by photopolymerization,” *Annual Review of Materials Research*, vol. 46, no. 1, pp. 19-40, 2016. doi: 10.1146/annurev-matsci-070115-031841.

[2] N. A. Chartrain, C. B Williams, and A. R. Whittington, “A review on fabricating tissue scaffolds using vat photopolymerization,” *Acta biomaterialia*, vol. 74, pp. 90-111, 2018. doi: 10.1016/j.actbio.2018.05.010.

[3] Q. Mu *et al.*, “Digital light processing 3D printing of conductive complex structures,” *Additive Manufacturing*, vol. 18, pp. 74-83, 2017. doi: 10.1016/j.addma.2017.08.011.

[4] S.H. Kim *et al.*, “Precisely printable and biocompatible silk fibroin bioink for digital light processing 3D printing,” *Nature communications*, vol. 9, no. 1, pg. 1-14, 2018. doi: 10.1038/s41467-018-03759-y.

[5] S. Tibbits, “4D printing: multi-material shape change,” *Architectural Design*, vol. 84, no. 1, pp. 116-121, 2014. doi: 10.1002/ad.1710.

[6] Z. Ding, C. Yuan, X. Peng, T. Wang, H. J. Qi, and M. L. Dunn, “Direct 4D printing via active composite materials,” *Science advances*, vol. 3, no. 4, pp. e1602890, 2017. doi: 10.1126/sciadv.1602890.

[7] L.R. Meza, S. Das, and J. R. Greer, “Strong, lightweight, and recoverable three-dimensional ceramic nanolattices,” *Science*, vol. 345, no. 6202, pp. 1322-1326, 2014. doi: 10.1126/science.1255908.

[8] X. Xia *et al.*, “Electrochemically reconfigurable architected materials,” *Nature*, vol. 573, no. 7773, pp. 205-213, 2019. doi: 10.1038/s41586-019-1538-z.

[9] M. Layani, X. Wang, and S. Magdassi, “Novel materials for 3D printing by photopolymerization,” *Advanced Materials*, vol. 30, no. 41, pp. 1706344, 2018. doi: 10.1002/adma.201706344.

[10] C. B. Arrington, D. A. Rau, C. B. Williams, and T. E. Long, “UV-assisted direct ink write printing of fully aromatic Poly(amide imide)s: Elucidating the influence of an acrylic scaffold,” *Polymer,* vol. 212, pp. 123306, 2021. doi: 10.1016/j.polymer.2020.123306.

[11] J. R. Tumbleston *et al.*, “Continuous liquid interface production of 3D objects,” *Science*, vol. 347, no. 6228, pp. 1349-1352, 2015. doi: 10.1126/science.aaa2397.

[12] R. Janusziewicz, J. R. Tumbleston, A. L. Quintanilla, S. J. Mecham, and J. M. DeSimone “Layerless fabrication with continuous liquid interface production,” *Proceedings of the National Academy of Sciences*, vol. 113, no. 42, pp. 11703-11708, 2016. doi: 10.1073/pnas.1605271113.

[13] J. G. Leprince, W. M. Palin, M. A. Hadis, J. Devaux, and G. Leloup, “Progress in dimethacrylate-based dental composite technology and curing efficiency,” *Dental Materials*, vol. 29, no. 2, pp. 139-156, 2013. doi: 10.1016/j.dental.2012.11.005.

[14] G. B. Brown, G. F. Currier, O. Kadioglu, and J. P. Kierl, “Accuracy of 3-dimensional printed dental models reconstructed from digital intraoral impressions,” *American Journal*

of Orthodontics and Dentofacial Orthopedics, vol. 154, no. 5, pp. 733-739, 2018. doi: 10.1016/j.ajodo.2018.06.009.

[15] Y. L. Yap and W. Y. Yeong "Additive manufacture of fashion and jewellery products: a mini review," *Virtual and Physical Prototyping*, vol. 9, no.3, pp.195-201, 2016. doi: 10.1080/17452759.2014.938993.

[16] D. K. Patel, A. H. Sakhaei, M. Layani, B. Zhang, Q. Ge, and S. Magdassi, "Highly stretchable and UV curable elastomers for digital light processing based 3D printing," *Advanced Materials*, vol. 29, no. 15, pp. 1606000, 2017. doi: 10.1002/adma.201606000.

[17] C. Decker, "The use of UV irradiation in polymerization," *Polymer International*, vol. 45, no. 2, pg. 133-141, 1998. doi: 10.1002/(SICI)1097-0126(199802)45:2<133::AID-PI969>3.0.CO;2-F.

[18] V. Shukla, M. Bajpai, D. K. Singh, M. Singh, and R. Shukla, "Review of basic chemistry of UV-curing technology," *Pigment & Resin Technology*, vol. 33, no.5, pp.272-279, 2004. doi: 10.1108/03699420410560461.

[19] C. Mendes-Felipe, J. Oliveira, I. Etxebarria, J. L. Vilas-Vilela, and S. Lanceros-Mendez, "State-of-the-art and future challenges of UV curable polymer-based smart materials for printing technologies," *Advanced Materials Technologies*, vol. 4, no. 3, pp. 1800618, 2019. doi: 10.1002/admt.201800618.

[20] L. Tytgat *et al.* , " Photo-crosslinkable recombinant collagen mimics for tissue engineering applications," *Journal of Materials Chemistry B*, vol. 7, no. 19, pp. 3100-3108, 2019. doi: 10.1039/C8TB03308K.

[21] Z. Zhao, J. Wu, X. Mu, H. Chen, H. J. Qi, and D. Fang, "Origami by frontal photopolymerization," *Science advances*, vol. 3, no. 4, pg. e1602326, 2017. doi: 10.1126/sciadv.1602326.

[22] K. T. Haraldsson, J. B. Hutchison, R. P.Sebra, B. T. Good, K. S. Anseth, and C. N. Bowman, "3D polymeric microfluidic device fabrication via contact liquid photolithographic polymerization (CLiPP)," *Sensors and Actuators B: Chemical*, vol. 113, no. 1, pp. 454-460, 2006. doi: 10.1016/j.snb.2005.03.096.

[23] B. K. Gale *et al.*, "A review of current methods in microfluidic device fabrication and future commercialization prospects," *Inventions*, vol. 3, no. 3, pp. 60, 2018. doi: 10.3390/inventions3030060.

[24] T. Rehbein, A. Lion, M. Johlitz, and A. Constantinescu, "Experimental investigation and modelling of the curing behaviour of photopolymers," *Polymer Testing*, vol. 83, pp. 106356, 2020. doi: 10.1016/j.polymertesting.2020.106356.

[25] J. W. Halloran et al., "Photopolymerization of powder suspensions for shaping ceramics," *Journal of the European Ceramic Society*, vol. 31, no. 14, pp. 2613-2619, 2011. doi: 10.1016/j.jeurceramsoc.2010.12.003.

[26] H. F. Brinson and L. C. Brinson, *Polymer Engineering Science and Viscoelasticity: An Introduction*. Springer New York, NY, 2008, pp. 181-191. doi: 10.1007/978-0-387-73861-1.

[27] M. Hossain, G. Possart, and P. Steinmann, "A small-strain model to simulate the curing of thermosets," *Computational Mechanics*, vol. 43, no. 6, pp. 769-779, 2009. doi: 10.1007/s00466-008-0344-5.B.

[28] Golaz, V. Michaud, Y. Leterrier, and J.A. Månson, " UV intensity, temperature and dark-curing effects in cationic photo-polymerization of a cycloaliphatic epoxy resin," *Polymer*, vol. 53, no. 10, pp. 2038-2048, 2012. doi: 10.1016/j.polymer.2012.03.025.

[29] M. R. Kamal, “Thermoset characterization for moldability analysis,” *Polymer Engineering & Science*, vol.14, no. 3, pp. 231-239, 1974. doi: 10.1002/pen.760140312.
[30] S. Sourour and M. R. Kamal, “Differential scanning calorimetry of epoxy cure: isothermal cure kinetics,” *Thermochimica Acta*, vol. 14, no. 1-2, pp. 41-59, 1976. doi: 10.1016/0040-6031(76)80056-1.
[31] A. Maffezzoli and R. Terzi, “Effect of irradiation intensity on the isothermal photopolymerization kinetics of acrylic resins for stereolithography,” *Thermochimica Acta*, vol. 321, no. 1-2, pp. 111-121, 1998. doi: 10.1016/S0040-6031(98)00448-1.
[32] Matlab User Manual, Online Documentation, 2022. Available at https://www.mathworks.com/help/.
[33] D. F. Swinehart, “The Beer-Lambert law,” *Journal of chemical education*, vol. 39, no. 7, pp. 333-335, 1962. doi: 10.1021/ed039p333.
[34] K. Sekmen, T. Rehbein, M. Johlitz, A. Lion, and A. Constantinescu, “Thermal analysis and shrinkage characterization of the photopolymers for DLP additive manufacturing processes,” *Continuum Mechanics and Thermodynamics*, 2022. doi: 10.1007/s00161-022-01137-0.
[35] T. Rehbein, M. Johlitz, A. Lion, K. Sekmen, and A. Constantinescu, “Temperature-and degree of cure-dependent viscoelastic properties of photopolymer resins used in digital light processing,” *Progress in Additive Manufacturing*, vol. 6, no. 4, pp. 743–756, 2021. doi: 10.1007/s40964-021-00194-2.
[36] ASTM D4473-08, Standard test method for plastics: Dynamic mechanical properties: Cure behavior, 2008.
[37] Y. Eom, L. Boogh, V. Michaud, P. Sunderland, and J. A. Månson, “Time-cure-temperature superposition for the prediction of instantaneous viscoelastic properties during cure,” *Polymer Engineering & Science,* vol. 40, no. 6, pp. 1281-1292, 2000. doi: 10.1002/pen.11256.